

## **Relative Study of Nonlinear Analysis for Torsional Strengthened RC Beams with Web Opening using CFRP and Steel Plates**

**Khaled Fawzy**

*Structural Engineering Dept., Faculty of Engineering, Zagazig University, Zagazig, Sharkia, Egypt*  
*Corresponding Author: Khaled Fawzy*

---

**Abstract:** *This paper displays the numerical study on fortifying reinforced concrete (RC) beams with opening exposed to unadulterated torsion. The finite elements implemented by ANSYS-2013 are used for this study. For the purpose of confirmation of the finite element model established, the numerical study is first carried out on the RC beam fortifying by external bonded-carbon fiber reinforced polymers (EB-CFRP) that were experimentally tested and described in the literature. Then the study has been stretched for the same RC beams fortifying with steel plates. The major parameter involved in this study is the fortifying effect of different schemes of steel plates and the plate's thickness on the behavior of RC beams with opening underneath torsion. The present study reveals that the finite element models can ascertain the structural behavior of the tested beams and can be an excellent alternative of damaging laboratory tests with acceptable results, and the steel plates are more effective in strengthening the RC beams compared to the strengthening with (CFRP) for some schemes. Also results have been compared with the design methodologies of some international codes and analytical procedure produced by previous researchers. Finally, a simple suggested equation is produced to inference the torsional moment capacity of a fortifying RC beam with opening. The proposed condition affirms the precision and viability of the finite element results.*

**Keywords:** *Nonlinear, Torsion, RC beams, CFRP, Steel plate.*

---

Date of Submission: 13-01-2018

Date of acceptance: 31-01-2018

---

### **I. Introduction**

The existences of transverse openings in floor beams are more often used to provide passage for utility duct and pipes. Due to the presence of a hole in the beam leads to cracks and weakness in stiffness, this leads to the requirement of fortifying such beams. Mansur [1 to 3] studied a series of RC beams, with a various size of rectangular openings having additional longitudinal reinforcement near to the upper and base edges of the opening, full-stirrups by the vertical edges and closed connections in both top and base chord individuals at the opening, Mansur concluded that after the beams are loaded, an initial diagonal cracks with approximately 45° appeared at the opening corners, any escalation in the opening length or depth decreases the cracking load, the eccentricity of the opening has no influence on the cracking torque. El-Badawy [4] tested eight opening RC beams beneath torsion and flexural moment to study the influence of position and detailing of reinforcement around the opening, results show that, web opening affects significantly on the beam strength, web opening height has a pronounced effect on the capacity than the opening width, post-cracking stiffness of the RC beams with opening under torsion is only about 25% of the pre-cracking stiffness of corresponding beam, and the additional reinforcement detailing and intensity around the web opening significantly affect torsion capacity of reinforced concrete beams. Lately, strengthening of reinforced concrete (RC) beams subjected to torsion is receiving increased attention, several researches have attentive on the influence of torsion on solid beam, Panchacharam [5] presented an experimental and analytical verification of the torsion behavior and performance of RC solid beams guaranteed with outside bonded GFRP sheets, the experimental study included some variables, the results show that both the cracking and the ultimate load are significant increased with externally bonded GFRP sheets, and a complete 90-degree wrap strengthening provides an effective confinement and therefore occasioned in a weighty increase the load by 150%. A lot of researchers studied numerically the pure torsional behavior [6 to 8], and combined flexural and torsional behavior of RC beams using the FEA method [9 to 11], but a fewer took the influence of the presence of transverse opening through the beam into account.

In this paper, the analysis of strengthening RC beams under torsion depends on the finite element method. The finite elements approved by ANSYS were used for this study. The numerical study on the behavior of strengthening RC beams that were experimentally tested and reported by Fawzy et al. [12] was first carried out to legalize the model developed in this study. This study was further been extended for the same reinforced concrete beams strengthening either with carbon fiber reinforced polymers (CFRP) or steel plates for comparison.

## II. Experimental Program

### 1. Specimen Details

A seven reinforced concrete beams, detailed in Figure 2, were tested in pure torsion. Two beams, with and without opening, were tested to be a control beams. Five of the seven beams were strengthened with various schemes of the external bonded (EB-CFRP) sheets [12]. As shown in Figure 1, the cross section dimension is 100 mm x 350 mm and the beam span is 1780 mm. The opening dimension for beam with opening is 150 mm height and 520 mm in length. The longitudinal reinforcement is taken to be 8 bars with 10 mm, four bars at the corners and the rest of the bars are placed close to the top and bottom edges of the opening. The shear reinforced for solid control beam are closed stirrups with 6 mm diameter spaced at 90 mm on center. Similar stirrups are utilized in the solid part for the beams with web opening notwithstanding utilizing a closed stirrups with 4 mm diameter dispersed at 40 mm on center in the top and base chords in the opening zone. To avert local failure; transverse stirrups with 6 mm bars and separated at 40 mm on center were utilized at the end of each beam.

### 2. Strengthening Schemes and Materials

A unidirectional carbon fiber fabric (SikaWrap-230C) with 0.131 mm per layer was used. The manufacturer's specified tensile strength modulus, tensile strength and its elongation at fibers failure were 238 GPa, 4300 MPa and 1.8%. The laminate thickness was about 0.35 mm. The tensile modulus of elasticity and strength on the basis of 1.0 mm of the laminate are 28 GPa and 350 MPa respectively. The impregnation of the fiber used is a two part, epoxy-based thixotropic impregnating resin / adhesive (Sikadur-330) with a density of 1.3 kg / l, modulus of elasticity 4500 MPa Tensile Strength 30 MPa.

### 3. Test set-up

Using a machine with 250 kN capacity, the beams were tested. The two holders of the individual carriers were transversely and freely rotate about the longitudinal beam axis of the supported, as displayed in Figure 3. All beams were tested under pure torsion on concentrated load on a rigid steel I-beam, the spreading of the load on two rigid steel arms terminating at the beam. Two weights having the same weight of the I-beam were utilized to disregard the effect of the weight of the I-beam during the charging process. The twisted angle of the beam was measured by the applied torque. Through the use of LVDT horizontal near the upper beam edge, Four LVDTs were distributed along the beam length to anti-symmetric positions at a distance of 400 mm and 600 mm from the center of the beam to ensure that the load is evenly distributed on the charged weapons of steel. To confirm next, the average value of the LVDTs acquired. Figure 3 displays the details of the steel shop, and the location of the LVDTs.

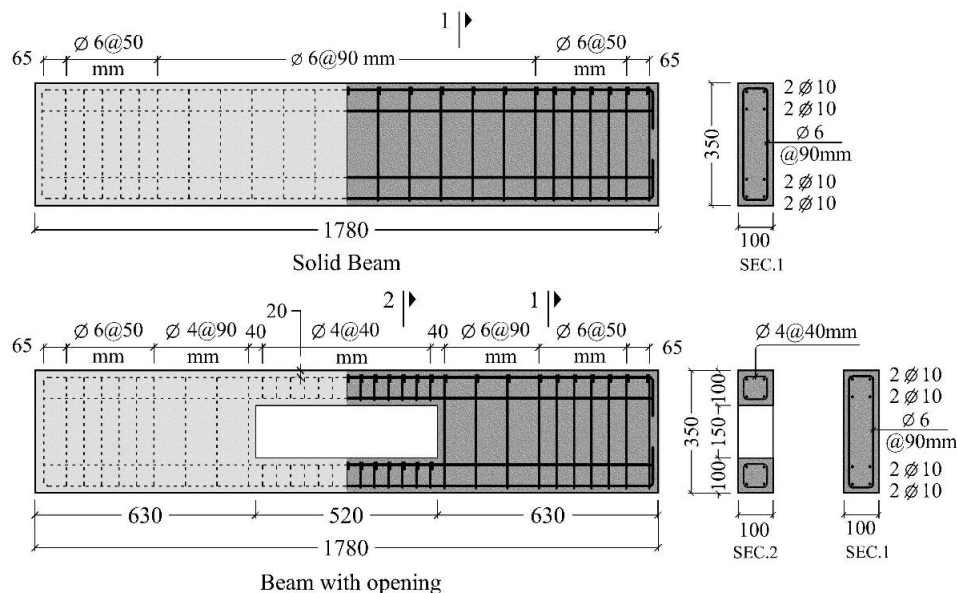


Fig. 1: Tested beams dimensions and reinforcement details.

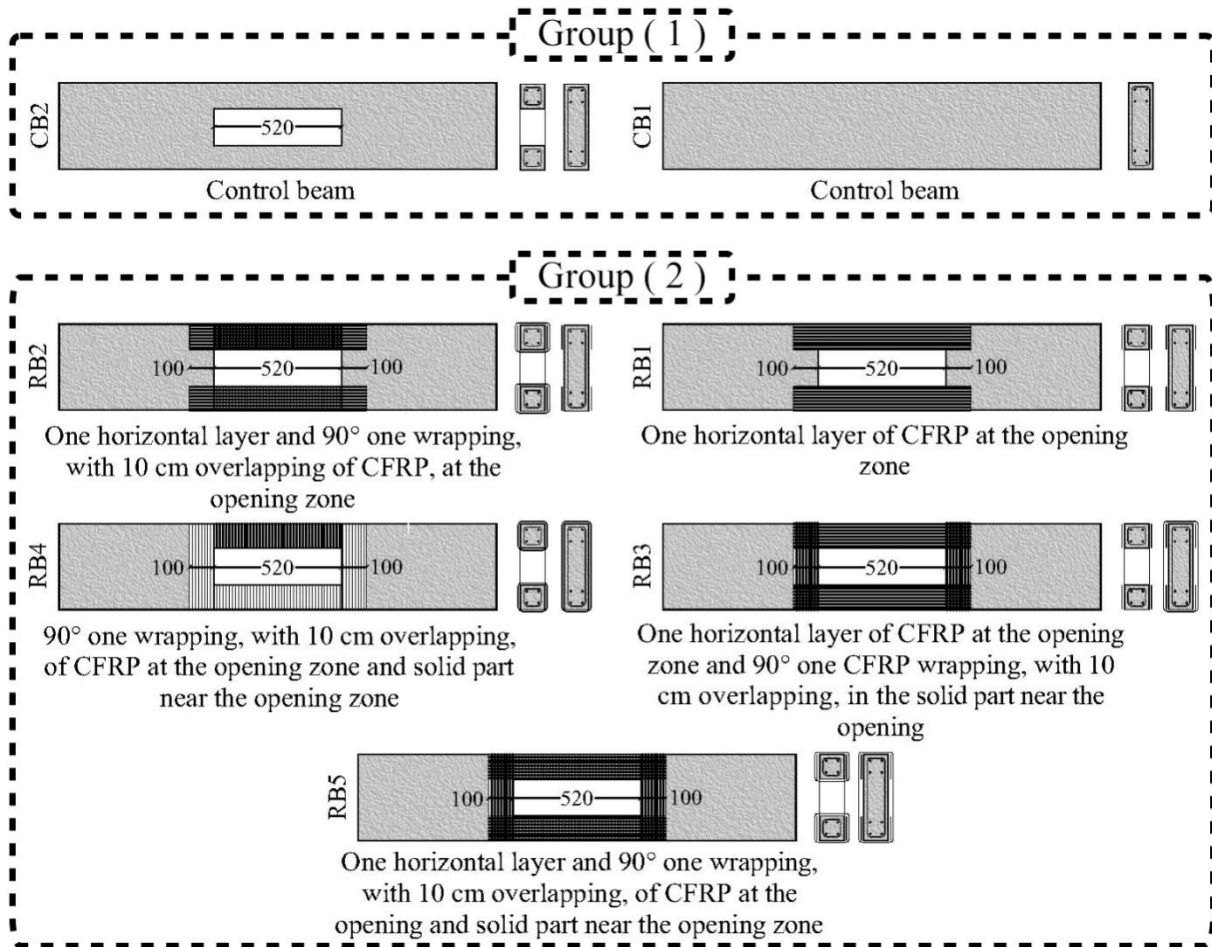


Fig. 2: Specimens details.

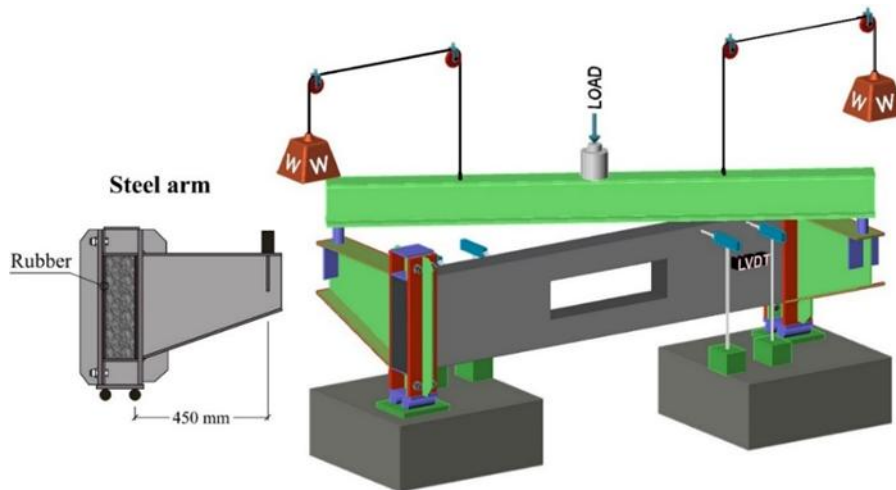


Fig. 3: Test setup and instrumentation.

### III. Finite Element Modeling

#### 1. Element type

Concrete and resin was modeled using 3-D 8-node solid element (**SOLID65**), this element is accomplished of cracking in tension and crushing in compression. Steel arm and CFRP composite were modeled using **SOLID185** element. A **LINK180** element is used to model steel reinforcement. A solid 45, a 3-D structural solid element was used to model the steel plates.

**2. Boundary conditions**

To confirm that the model acts the same way as the experimental beams, boundary conditions need to be applied at supports and points of anti-symmetry to increase the beam constrain; which give a better results in convergence solution. The nodal displacement load is used to model the boundary condition in this ANSYS models. The supports were modeled in such a way that rollers were created. A single node in the center of the support part was given a constraint in the UX and UY equal zero; consequently, the steel arm will be allowed to rotate in X, Y, and Z directions and translate in Z direction at every support. The beam was obstructed to translate in Z direction using the anti-symmetry boundary condition. As shown in Fig. 3 the load was applied as a vertical displacement in Y direction instead of forcing load to get a good representation of the curves after the peak point. The boundary conditions for both planes of anti-symmetry and support are shown in Fig. 4.

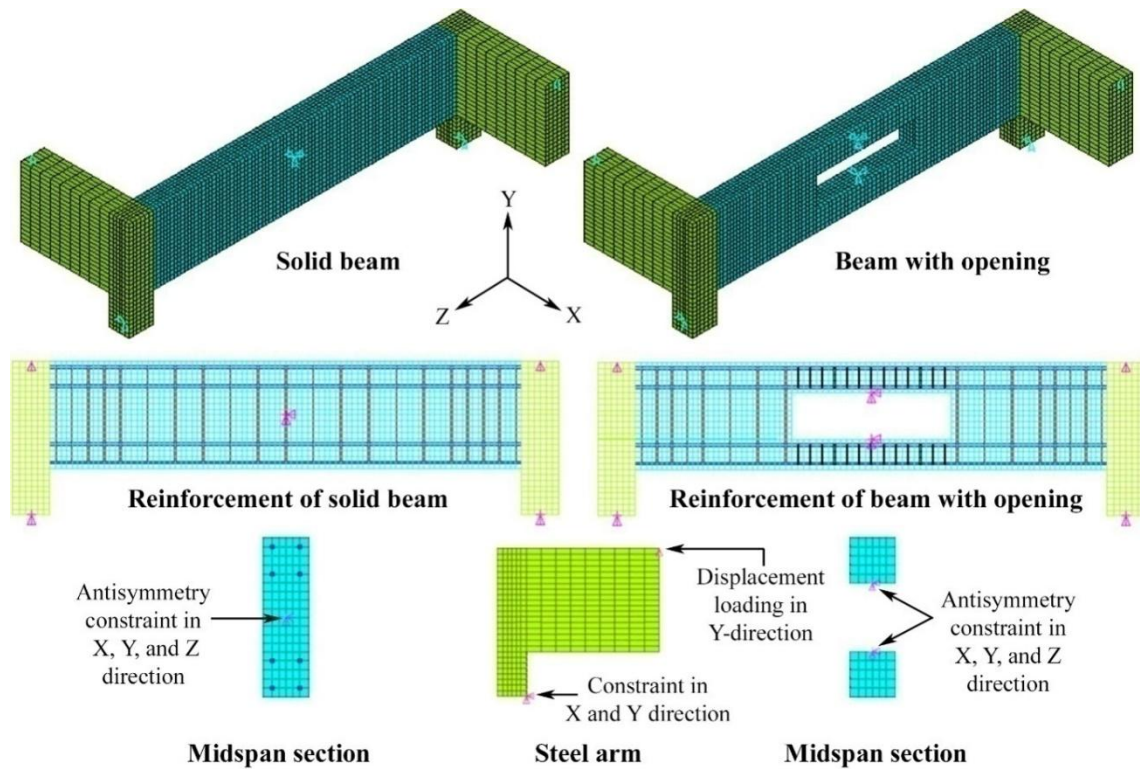


**Fig. 4: meshing reinforcement arrangement, and boundary condition of solid beam and beam with opening.**

**IV. Comparison AND DISCUSSION**

**1. Comparison with experimental results**

The failure bending and twisting moments for the control beams obtained from the numerical study were matched with the experimental results reported by Fawzy et al. [12], and are presented in table 1 and Figs (5 -10). From the Table 1, it is seen that the results show good agreement when compared with the experimental results and the maximum error is not exceeded 20%. For all beams, it exhibited similar linear torque-rotation behavior from initial loading up to the occurrence of the initial crack. After the formation of the cracks, all beams showed nonlinear behavior. Just the initial cracking occurred, the strengthened beams tends to be stiffer than the reference CB2 beam with varying degrees according to the strengthening type. Using of the CFRP resulted in increasing the ultimate capacity of the beams at different rates depending on the method of strengthening.

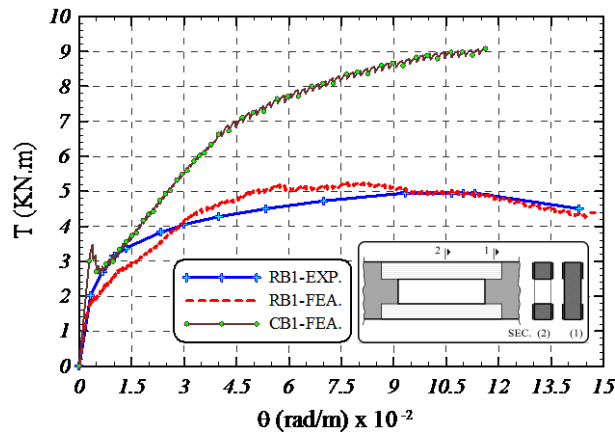


Fig. 5: Torque versus twist angle per meter for beam (RB1) and reference beams (CB1).

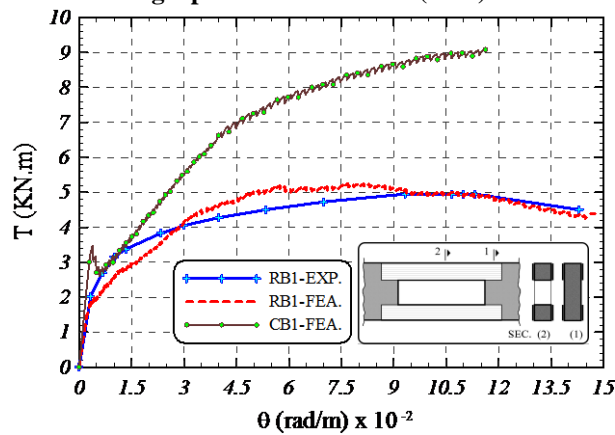


Fig. 6: Torque versus twist angle per meter for beam (RB2) and reference beams (CB1).

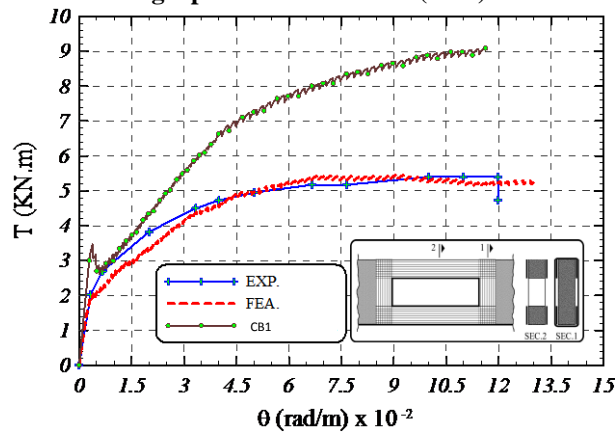


Fig. 7: Torque versus twist angle per meter for beam (RB3) and reference beams (CB1).

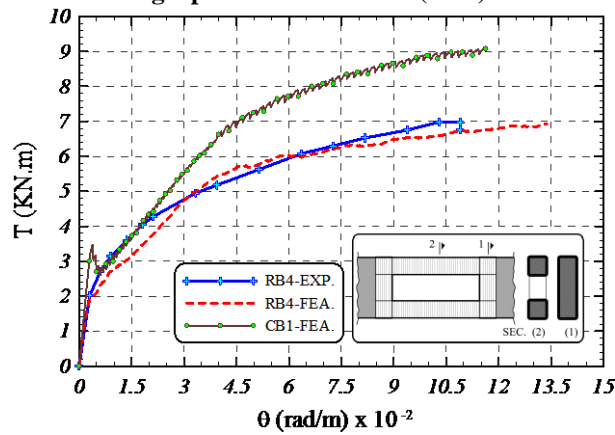


Fig. 8: Torque versus twist angle per meter for beam (RB4) and reference beams (CB1).

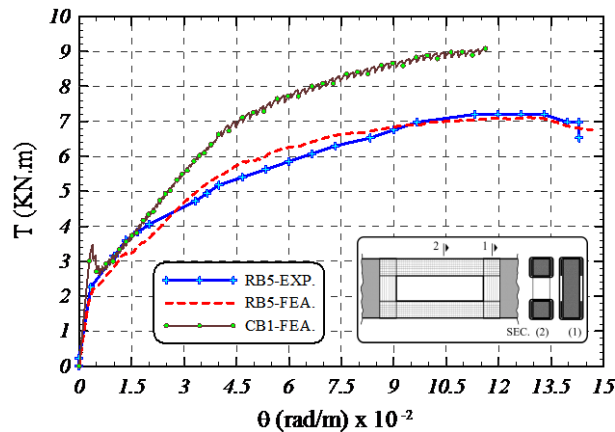


Fig. 9: Torque versus twist angle per meter for beam (RB5) and reference beams (CB1).

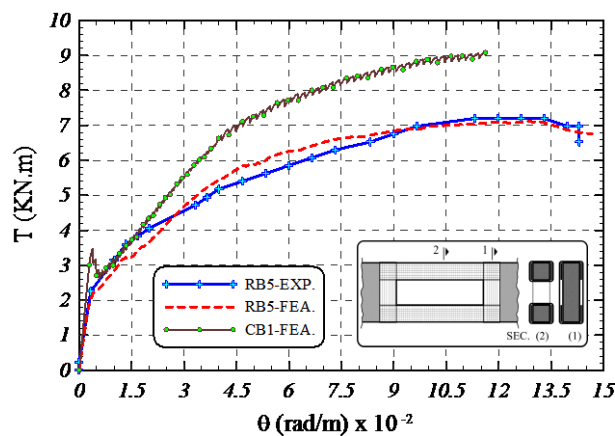


Fig. 10: Torque versus twist angle per meter for beam (RB5) and reference beams (CB1).

Table 1: Experimental and finite element analysis results tests (strengthened with CFRP)

Beam Symbol	Results at Cracking Torque					Results at Ultimate Torque				
	Applied Torque		$\frac{T_{FEA}}{T_{EXP}}$	Angle of Twist		Applied Torque		$\frac{T_{FEA}}{T_{EXP}}$	Angle of Twist	
	kN.m			rad/m x10-3		kN.m			rad/m x10-3	
	Exp.	FEA.	Exp.	FEA.	Exp.	FEA.	Exp.	FEA.		
CB1	3.15	3.47	1.10	3.33	3.80	7.65	9.09	1.19	89.91	116.20
CB2	1.80	1.85	1.03	3.33	3.86	4.73	4.91	1.04	94.90	66.04
RB1	2.03	1.93	0.95	3.33	3.64	4.95	5.25	1.06	93.25	78.44
RB2	2.03	2.03	1.00	3.33	3.54	5.40	6.51	1.21	99.88	105.94
RB3	2.03	2.05	0.99	3.33	4.08	5.40	5.47	1.01	99.88	91.06
RB4	2.03	2.05	1.01	3.03	3.98	6.98	6.93	0.99	102.90	132.67
RB5	2.25	2.20	0.98	3.33	3.92	7.20	7.12	0.99	113.16	128.35

## 2. Control beams

The control beams, which represent the first group, contain solid beam (CB1), and beam with opening (CB2). For CB1 beam, the first crack appeared at the midpoint of the deeper face of the beam, and propagate diagonally with 45° towards the other smaller faces forming continuous helical cracks, the beam failed due to excessive increase in the diagonal crack of the deeper face. For CB2 beam, the initial cracks appeared at the corners of the opening in the tension side. After that, the cracks propagate diagonally towards the solid section. At this time, spiral continuous diagonal cracks with 45° appeared in the top and bottom chords. At later stage of the loading, diagonal cracks initiated in the solid part. The beam failed due to the failure of the top chord in middle part. The initiation of cracking of concrete for CB2 beam was at a torque of 1.85kN.m, with decreasing in the cracking torque ( $T_{cr}$ ) by a 47 % of the solid control beam which begin to crack at the cracking torque

(T<sub>cr</sub>) 3.47 kN.m. The angle of rotation at first crack ( $\theta_{cr}$ ) was  $3.80 \times 10^{-3}$  rad/m and  $3.86 \times 10^{-3}$  rad/m for CB1 and CB2 respectively. The solid and the beam with opening failed at ultimate torque (T<sub>ult</sub>) of 9.09 kN.m and 4.91 kN.m respectively, the percentage of decreasing in ultimate torque (T<sub>ult</sub>) of the beam with opening (CB2) was 46 % with respect to the solid beam (CB1), the angle of rotation per meter at failure ( $\theta_{ult}$ ) was  $3.80 \times 10^{-3}$  rad/m and  $3.84 \times 10^{-3}$  rad/m for CB1 and CB2, respectively. Fig. 11 shows the mode of failure for reference beams.

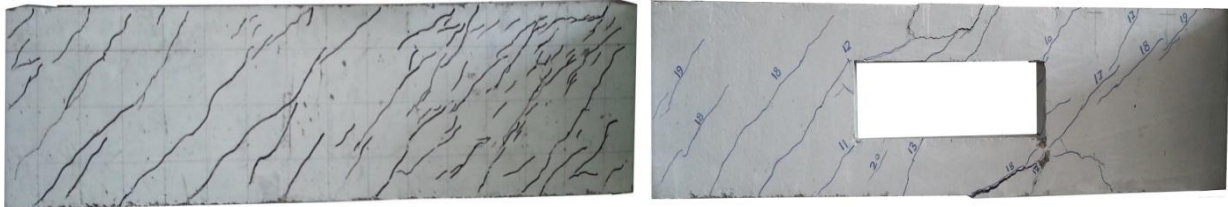


**Fig. 11: Crack pattern and mode of failure for reference beam (CB1 and CB2)**

### **3. Strengthened beams**

The second group contains the strengthened beams. The strengthened beams that have been modeled using ANSYS program are RB1, RB2, RB3, RB4, and RB5 as listed in Table **Error! Reference source not found.**1. The failure mechanism of each strengthened beam depended on the strengthening schemes. The numerical models were contrasted and the outcomes acquired from the experimental work. The outcomes were observed to be in a decent concurrence with the test comes about; however, significant deviations are seen between the experimental and numerical curves at ultimate stage for beam (RB2). It is presumed that during the actual testing there may be relaxation of constituent materials, whereas this type of relaxation will not occur in a pure numerical solution. All strengthened beams have nearly closed values of the initial cracking torque, which was ranged from 1.93 to 2.2 kN.m, which are shown in Table 1. RB1 and RB3 failed due to the failure of the top chord in middle part, they show slight increase in the ultimate torque by 7 % and 11.4 % of the ultimate torque of CB2 beam and 42% and 40% decrease of CB1 ultimate torque, respectively. The RB2 beam failed due to the formation of what called plastic hinges at the end of each chord. This beam was recorded 32.5 % increase in T<sub>ult</sub> of CB2 and 28.4% decreased of CB1 ultimate torque. The best strengthening schemes were for RB4 and RB5 beams which recorded increasing 0 in the ultimate torque, with respect to CB2 beam, by 41 % and 45 %, respectively, and approached the value of CB1 ultimate torque by 23.7% and 21.7% decrease, respectively.

### **4. Effect of fiber orientation**

Table 1 demonstrates the impact of fiber introduction on the torsional conduct of the RC beams strengthened with CFRP sheets. Cracking and ultimate torsional moment of the RC beam was increased slightly when it was strengthened with horizontal CFRP fibers (RB1, RB2, and RB3), whereas the ultimate torsional moment of the RC beam was increased significantly when it was strengthened with 90-degree GFRP fibers (RB3, and RB4). In Test beam with 90-degree CFRP fibers, failure mode was controlled by CFRP rupture. Whereas, in the test beam with horizontal CFRP fibers, the diagonal tensile stresses induced in the beam causes the CFRP sheet to separation in bundles of fibers. Generally, the 90-degree complete wrapping pattern provided an efficient confinement and in turn a significant increase in ultimate strength was observed.

Fig.s (12 -15) show the 3rd principle stress of the RC beams and the 1st principle stress of the CFRP sheets for all strengthened beams RB4 and RB5.

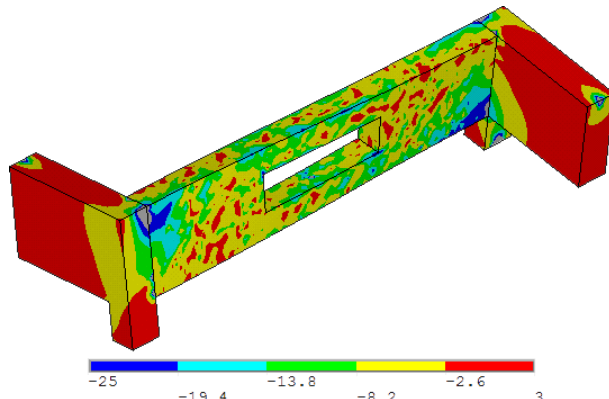


Fig. 12: 3rd principles stresses for beam (RB4) at ultimate torque

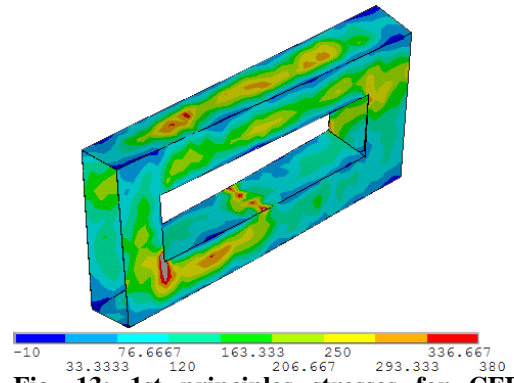


Fig. 13: 1st principles stresses for CFRP sheets of beam (RB4) at ultimate torque

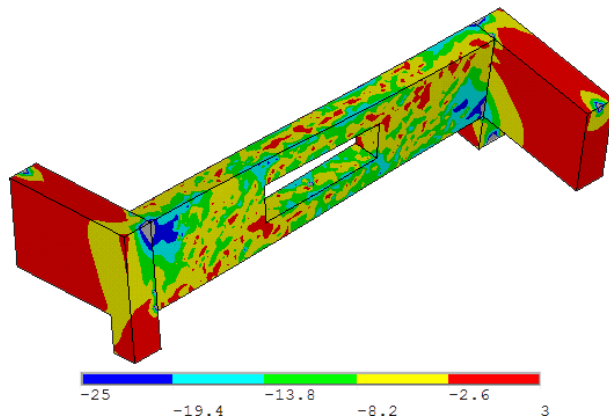


Fig. 14: 3rd principles stresses for beam (RB5) at ultimate torque

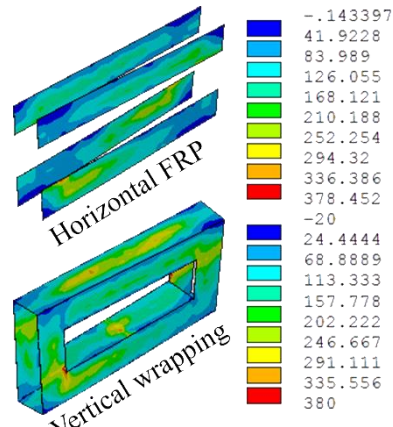


Fig. 15: 1st principles stresses for CFRP sheets of beam (RB5) at ultimate torque

### 5. Strengthening of beams using steel plates

Due to the orthotropic properties of the unidirectional composite lamina CFRP; the composite is very strong in the fiber direction and gives a poor properties in perpendicular direction, the test beam with horizontal CFRP fiber orientation exhibited a maximum (58 %) of ultimate torque capacity of solid beam (CB1) among all the test beams as shown in Table 2. However, the largest ultimate torque capacity is (76 %) of (CB1) for the test beam strengthened with fibers in 90-degree direction (Table 2). To overcome this problem, the numerical study is extended RC beams strengthened with steel plates instead of CFRP sheets. Two of the tested strengthened beams with steel plate having two different thicknesses of 2.0 mm and 4.0 mm with similar modeling shape for each of specimen RB1, RB3, and RB4 are presented and discussed. The elastic modulus and yield strength were taken as  $2 \times 10^5$  MPa and 400 MPa, respectively with poison ratio of 0.3. The same resin material with thickness of 1.0 mm has been used.

The torsional moment-rotation behavior of strengthened beams with CFRP sheets and steel plates for RB1, RB3, and RB4 models along with reference beam CB1 are plotted in Figs (16-18). The deformational conduct considered accentuation connection between the torsional moments carried by the test specimen against the maximum twist angle of the specimen cross section which has found the maximum twist angle of reference beam CB1, CB2 to be 0.1162 and 0.066 rad/m respectively at ultimate torsional moment 9.09 and 4.91 KN m respectively, the ultimate torsional moment strengthened with CFRP has found 5.25, 5.47, and 6.93 KN. m for RB1, RB3, and RB4 models respectively, and the maximum twist angle equal 0.145, 0.13, and 0.1325 rad/m respectively. The rotational capacity of RB1, RB3, and RB4 increased by 2.19, 1.97, and 2.01 respectively times over the CB2.

The ultimate torsional moment strengthened with steel plate 2 mm has found 6.7, 7.82, and 9.77 KN. m for RB1, RB3, and RB4 models respectively, and the maximum twist angle equal 0.1425, 0.14, and 0.145 rad/m respectively. The rotational capacity of RB1, RB3, and RB4 increased by 2.159, 2.12, and 2.19 respectively times over the CB2. There is no such significant variation in the rotational capacity values with variation of strengthened material type.



The ultimate torsional moment, the Torsional toughness and the ratio of torsional moment strengthened with CFRP sheets and steel plates for different models to corresponding torsional moment of reference beams CB2 and CB1 are listed in table 2.

Using of steel plate with thicknesses 4.0 mm for strengthening, leads to the same results of improvement in ultimate torsional strength for steel plate with 2mm thicknesses (Table 3), due to the failure of resin material. The ultimate torsional strength for RB1, RB3, and RB4 models was increased by 27.6 %, 43 %, and 41 %, respectively with steel thicknesses 2.0 mm, with respect to strengthened beams with CFRP. When comparing the ultimate torsional moment with that of reference beam, it turned out that, this technique led to increase in the ultimate torsional strength by 37 %, 59 %, and 99 %, respectively, with respect to torsional moment capacity of CB2 beam, and to reached to 74%, 86 %, and 107 %, respectively, of torsional moment capacity of CB1 beam.

Torsional toughness of the members is indicated by the area under torque twist response. For strengthened beams with CFRP, the toughness is found to be 0.624kNm/m, 0.56 kNm/m and 0.675 kNm/m for RB1, RB3, and RB4 models respectively. The ratios of toughness of these beams with respect to reference beam CB2 are found to be 1.66, 1.49 and 1.8, respectively. For strengthened beams with steel plate 2mm, the toughness is found to be 0.71 kNm/m, 0.885 kNm/m and 1.05 kNm/m for RB1, RB3, and RB4 models respectively. The ratios of toughness of these beams with respect to reference beam CB2 are found to be 1.89, 2.36 and 2.8, respectively. The toughness is improved with using steel plate for strengthening; the toughness of beams using strengthening steel plate is increased over the beams using strengthening CFRP by 1.14, 1.58, and 1.56 for of RB1, RB3, and RB4 respectively.

The cracking torsional moment ( $T_{cr}$ ), the ultimate torsional moment ( $T_{ult}$ ), and the rotational ductility index ( $\mu_T$ ) for strengthened with CFRP sheets and steel plates for different are listed in table 3.

The rotational ductility index is presented, for a thorough evaluation of the strengthening influence on the reaction and for comparison reasons of test results in terms of ductility. Rotational ductility index ( $\mu_T$ ) is expressed as the ratio of twist at maximum torque ( $\Theta_{max}$ ) to twist at cracking torque ( $\Theta_{Tcr}$ ) [19]. The ductility index for control specimen (CB2) without strengthening is found to be 16.92. For strengthened beams with CFRP, the ductility index is increased and found to be 21.67, 22.19, and 33.84 for RB1, RB3, and RB4 models respectively. For strengthened beams with steel plate 2mm, the ductility index is decreased and found to be 11.54, 7.45, and 5.71 for RB1, RB3, and RB4 models respectively.

The initial stiffness of these beams are same as their control specimen (CB2) before cracking, but there is reduction in the stiffness at ultimate torque which allowed the beams for great rotations. This denotes that there strengthening improves the rotational capacity of the beams. The stiffness at ultimate torque of strengthening beams using steel plate descends hastily compared to strengthening using CFRP.

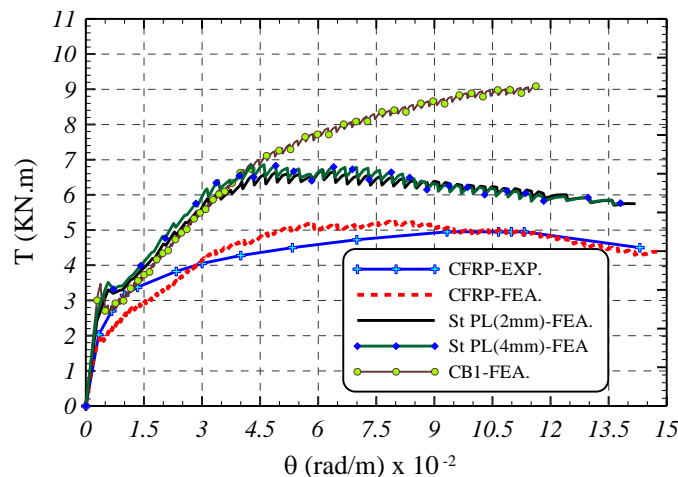


Fig. 16: Torque versus twist angle per meter for beam (RB1) and reference beams (CB1)

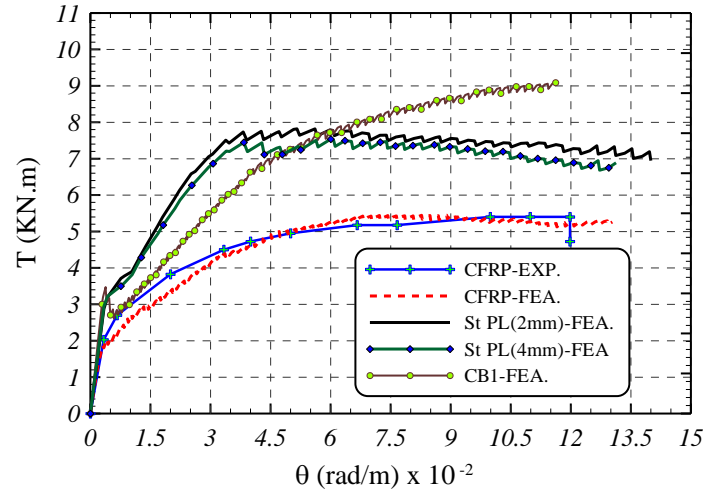


Fig. 17: Torque versus twist angle per meter for beam (RB3) and reference beams (CB1)

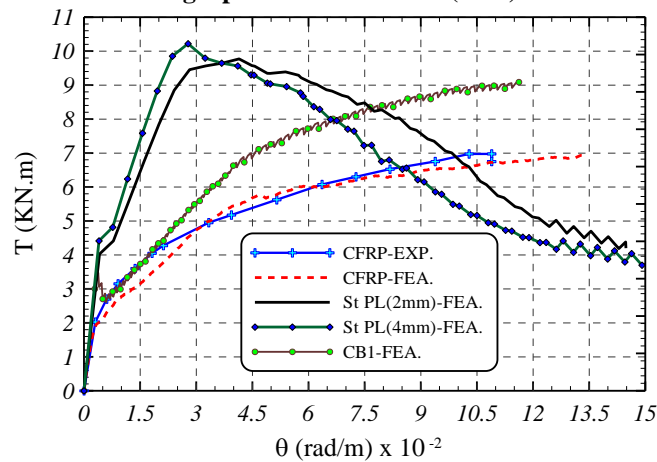


Fig. 18: Torque versus twist angle per meter for beam (RB4) and reference beams (CB1)

Table 2: Comparison between FEA results of CFRP and steel plate strengthening (2mm- 4 mm).

Beam Symbol	CFRP				ST PL.2mm (4mm)			
	Tult, (kN.m)	$\frac{T_{ult RB}}{T_{ult CB2}}$	$\frac{T_{ult RB}}{T_{ult CB1}}$	toughness	Tult, (kN.m)	$\frac{T_{ult RB}}{T_{ult CB2}}$	$\frac{T_{ult RB}}{T_{ult CB1}}$	toughness
CB2	4.91	Without strengthening		0.375	4.91	Without strengthening		0.375
RB1	5.25	1.07	0.58	0.624	6.70 (6.7)	1.37 (1.37)	0.74 (0.74)	0.71
RB3	5.47	1.12	0.60	0.56	7.82 (7.61)	1.59 (1.55)	0.86 (0.84)	0.885
RB4	6.93	1.41	0.76	0.675	9.77 (9.65)	1.99 (1.96)	1.07 (1.066)	1.05

Table 3: Comparison between FEA results of CFRP and steel plate strengthening (2mm).

Beam Symbol	CFRP					ST PL.2mm				
	Tcr, (kN.m)	ThetaTcr	Tult, (kN.m)	Theta max	muT	Tcr, (kN.m)	ThetaTcr	Tult, (kN.m)	Theta max	muT
CB2	Without strengthening Tcr, = 1.85 ThetaTcr = .0039 Tult, = 4.91 Theta max = .066 muT = 16.92									
RB1	1.93	.0036	5.25	.078	21.67	2.8	.0039	6.70	.045	11.54
RB3	2.05	.0041	5.47	.091	22.19	3.1	.0047	7.82	.035	7.45
RB4	2.05	.0039	6.93	.132	33.84	4.1	.0049	9.77	.028	5.71

**6. Torsional moment predication using international codes**

The design for torsion in best codes is based on a thin-walled tube, space truss analogy. A beam subjected to torsion is idealized as a thin-walled tube abandoning the core of the solid concrete section. Once a reinforced concrete beam has cracked in torsion, its torsional resistance is provided mainly by closed stirrups and longitudinal bars located close the surface of the member. In this paper, the torsional moment capacity for solid control beam has been calculated using ECP 203-09 [21], ACI 318-05 [22], BS8110-97 [23], and JSCE-07 [24]. The codes results compared with the finite element values and tabulated in Table 4 and Table 5.

**7. Nominal torsional moment for beam with large rectangular opening**

Mansur & Tan [2] used an analytical method to calculate the nominal torsional moment for reinforced concrete beam with large rectangular opening (Tn) based on the collapse load analysis. Using this method, the authors expressed two solutions, the upper and lower bound solution, to get the nominal torsional moment. In this section, the lower bound solution (LBS) for identical chord is used, as the mechanism is missed. The LBS consists of three mode 1, 2, and 3 depending on the position of compression zone in the section. As the mode failure of CB2 beam identical with mode 1 failure, where the compression failure zone located in the upper face of the upper chord section, then the value of torsional moment capacity can be calculated according to equation (1).

$$T_n = t_n T_o \tag{1}$$

$$t_n = \frac{-\alpha \beta}{2r} + \frac{1}{2} r \sqrt{(\beta^2 + 4r)(\alpha^2 + 4)} \tag{2}$$

Where  $\alpha = \alpha_{t,b} + \alpha_{t,b} / \omega$ ,  $\beta = 0.5 V_o l_o / M_o$ , and  $r = 1$  and  $\alpha_{t,b} = e V_o / T_o$ ,  $\omega = 1.0$ ,  $e$  is the spacing between centerline of top or bottom chord to the centerline of the solid cross section.

$$V_o = 2 \sqrt{\frac{2 F_{yu} S_y d_v}{s}} \tag{3}$$

$$T_o = 2 A_o \sqrt{\frac{4 F_{yu} S_y}{u s}} \tag{4}$$

Where  $F_{yu}$  is the yield force in longitudinal tension bars,  $S_y$  is the yield force in vertical stirrups,  $d_v$  is the spacing between longitudinal tension and compression bars,  $s$  is the spacing between stirrups,  $u$  is the perimeter of centerline connecting longitudinal bars in corner,  $A_o$  is the area enclosed by  $u$ ,  $l_o$  is the opening length, and  $M_o = 2 F_{yu} d_v$ .

**8. Torsion contribution of CFRP complete wrapping to the torsional capacity of beam with rectangular opening**

Using the Equations that calculate the torsion contribution of CFRP sheets to the torsional capacity of a solid beam which introduced by FIB [20] with some modification, as shown in Fig. (19), to match with beam with rectangular opening and the axis of rotation apart 150 mm from the bottom of the beam, then the torsion contribution of steel sheet can be derived as shown in equation (10) through equation (13).

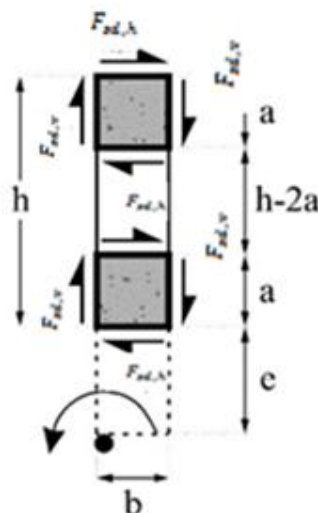


**Fig. 19:** Tensile force carried by steel sheet complete wrapping on the chords due to torsional moment

$$T_{sd} = 2F_{sd,v} (b) + 2F_{sd,h} (a) \tag{5}$$

And

$$F_{sd,v} = \varepsilon_{sd,e} E_{su} \frac{t_s b_s}{S_s} a \cot \theta \tag{6}$$

$$F_{sd,h} = \varepsilon_{sd,e} E_{su} \frac{t_s b_s}{S_s} b \cot \theta \tag{7}$$

Then  $T_{sd}$  can be expressed as

$$T_{sd} = 2 \left[ 2 \varepsilon_{sd,e} E_{su} \frac{t_s b_s}{S_s} (a b) \cot \theta \right] \tag{8}$$

which implies that  $T_{sd} = 2 T_{sd,v} = 2 T_{sd,h}$ . Therefore, the torsion contribution of steel, on the two chords, to the torsional capacity of the beam when the section rotate about a point apart 150 mm from the bottom of the beam is equal to the sum of the torsion contribution of steel, on the one chord, to the torsional capacity of the chord when it rotate about its centroid.

Where  $F_{sd,h}$  and  $F_{sd,v}$  are define as the forces carried by horizontal and vertical steel sheets, respectively,  $\varepsilon_{sd,e}$  is the characteristic value of steel strain and can be calculated for steel from equation (9),  $E_{su}$  is the elastic modulus of steel,  $t_s$  is the thickness of steel,  $b_s$  width of steel strip,  $S_s$  is the spacing between strips,  $\theta$  is the angle of inclination of the diagonal crack to the longitudinal axis of the beam, and can be taken as  $45^\circ$ , and

$$\varepsilon_{sd,e} = 0.17 \left[ \frac{f_{cm}^{(2/3)}}{E_{su} \rho_s} \right]^{0.3} \varepsilon_{su} \tag{9}$$

Where  $\varepsilon_{su}$  is the ultimate strain of steel,  $f_{cm}$  is defined as the concrete compressive strength, MPa,  $E_{su}$  is the elastic modulus of steel, GPa, and  $\rho_s$  is the steel reinforcement ratio with respect to concrete and can be calculated as:

$$\rho_s = \frac{2 t_s b_s}{b S_s} \tag{1}$$

For complete wrapping ( $b_s / S_s = 1.0$ )

The torsional capacity (T) of beam with rectangular opening retrofitted with complete wrapping of steel, as in RB3, equal to the contribution of torsional moment produced by Mansur and steel equations and can be given as;

$$\begin{aligned} T &= T_n + T_{sd} \\ &= T_o \left[ \frac{-\alpha \beta}{2 r} + \frac{1}{2} r \sqrt{(\beta^2 + 4 r)(\alpha^2 + 4)} \right] \\ &\quad + 2 \left[ 2 \varepsilon_{sd,e} E_{su} \frac{t_s b_s}{S_s} (a b) \cot \theta \right] \end{aligned} \tag{2}$$

Table 4: Torsional strength according to standards predictions, experimental results.

CB1	TFE	TECP	TACI	TBS	TJSCE
	7.65	3.973	3.973	4.067	8.592
CB2	TFE	TMT			
	4.91	5.491			
RB	TFE	TMT + TSIB			
RB1	6.70	7.712			
RB3	7.82	7.711			
RB4	9.77	12.369			

Table 5: Comparison of the ultimate torques between standards predictions, experimental results.

CB1	$\frac{T_{TECP}}{T_{FE}}$	$\frac{T_{TACI}}{T_{FE}}$	$\frac{T_{TBS}}{T_{FE}}$	$\frac{T_{TJSCE}}{T_{FE}}$
	0.437	0.437	0.446	0.943
CB2	$\frac{T_{TMT}}{T_{FE}}$			

	1.119
<b>RB</b>	$\frac{(T_{MT} + T_{SIB})}{T_{FE}}$
<b>RB1</b>	1.151
<b>RB3</b>	0.986
<b>RB4</b>	1.266

### V. Conclusion

- 1- A numerical FEA models using ANSYS program were conducted to study the torsional behavior of reinforced concrete beams with CFRP and steel plates strengthening. The numerical models were compared with the results obtained from an experimental work. The results were found to be in a good agreement with the experimental results. The numerical modeling allows for a realistic modeling of the elastic and the post-cracking response of FRP strengthened RC beams under torsion and predicts with satisfactory accuracy the torsional moment at cracking and the ultimate torque capacity.
- 2- Strengthening of opening using steel plate is more efficient than the CFRP sheets, for the strengthening schemes where the fibers are perpendicular to the principle stresses resulted from torsional moment.
- 3- Toughness of beams using strengthening steel plate is slightly more than that of beams strengthening with CFRP, whereas the ductility index of beams strengthening with CFRP is more prominent than that of beams strengthening steel plate.
- 4- The stiffness at ultimate torque of strengthening beams using steel plate descends hastily compared to strengthening using CFRP.
- 5- The most effective strengthening scheme is though the steel plates covers the whole sides of the top, bottom chords and the solid part besides the opening, and is reached to the solid beam capacity.
- 6- The torsional moment capacity for reinforced concrete beam with web opening calculated by Mansur & Tan [2] can be modified to take the effect of steel plate strengthening.
- 7- The torsional moment capacity produced by Mansur and FIB equations give a good agreement with the finite elements results for both strengthening with CFRP and steel plates.

### References

- [1] M. A. Mansur, and A. Hasnat, Concrete beams with small openings under torsion, *Journal of the Structural Division, ASCE*, vol. 106, no. 11, 1979, pp. 2433-2447, Nov.
- [2] M. A. Mansur, and K. H. Tan, Concrete Beam with Opening Analysis and Design, U.S.: CRC Press LLC, 1999.
- [3] M. A. Mansur, P. Paramasivam, and S. L. Lee, Torsional Behavior of RC Beams with Web Opening, *International Journal of Structures*, vol. 2, no. 3, 1982, pp. 89-98, July - Sept.
- [4] M. A. El-Badawy, A. S. Essawy, A. H. Khalil, Torsion in reinforced concrete beams containing circular opening, M.Sc., AIN SHAMS University, CAIRO, 2010.
- [5] Panchacharam, S., and Belarbi, A., Torsional Behavior of Reinforced Concrete Beams Strengthened with FRP Composites, in *First Congress, Osaka, Japan, 2002, PP. 1-11*.
- [6] Ameli, M., Ronagh, H. R., & Dux, P. F., Behavior of FRP strengthened reinforced concrete beams under torsion, *Journal of Composites for Construction*, 11(2), 2007, 192-200.
- [7] Mahmood, M. N., Nonlinear analysis of reinforced concrete beams under pure torsion, *Journal of Applied Sciences*, 7(22), 2007, 3524-3529.
- [8] Kamiński, M., & Pawlak, W., Load capacity and stiffness of angular cross section reinforced concrete beams under torsion, *Archives of Civil and Mechanical En*, 2011.
- [9] El-Awady, E., Husain, M., & Mandour, S., FRP-Reinforced Concrete Beams Under Combined Torsion and Flex, 2013.
- [10] Shaarbaf, I. A. S., Three-dimensional non-linear finite element analysis of reinforced concrete beams in torsion, (*Doctoral dissertation, University of Bradford*), 1990.
- [11] Santhakumar, R., Dhanaraj, R., & Chandrasekaran, E., Behavior of retrofitted reinforced concrete beams under combined bending and torsion, a numerical study. *Electronic Journal of Structural Engineering*, 7, 2007, 1-7.
- [12] Fawzy, K. Hashem, M.M. Elnady, A.M., Performance Of RC Beams with Web Opening Subjected to Pure Torsion Strengthened with CFRP, *International Journal of Engineering and Innovative Technology (IJEIT)*, Volume 4, Issue 1, July 2014.
- [13] Desayi, P. and S. Krishnan, Equation for the Stress-Strain Curve of Concrete, *Journal of the American Concrete Institute*, 61, pp. 345-350, 1964, March.
- [14] ECP 203-2007, The Egyptian Code for Design and Construction of Concrete Structures, *Ministry of Housing, Cairo, Egypt, (In Arabic)*.
- [15] Kachlakev, D., Miller, T., Yim, S., Chansawat, K., & Potisuk, T., Finite Element Modeling of Concrete Structures Strengthened with FRP Laminates, *Final report, SPR*, 316, 2001.
- [16] Potisuk, T., Finite element modeling of reinforced concrete beams externally strengthened by FRP composites, 2000.
- [17] ACI Committee 440, State-of-the-Art Report on Fiber Reinforced Plastic Reinforcement for Concrete Structures, *American Concrete Institute, Farmington Hills, Michigan, February 1996*, p 68.
- [18] Dejke, V., Durability of FRP Reinforcement in Concrete. Literature Review and Experiments, *Licentiate thesis, Chalmers.*, 2001, 211 pp.
- [19] Chaliotis, C.E., Karayannis, C.G., Effectiveness of the use of steel fibres on the torsional behavior of flanged concrete beams, *Cem.Concr.Compos.*31 (5), 2009, 331-341.

- [20] *FIB, Federation Internationale du Beton, Externally bonded FRP reinforcement for RC structures, The International Federation for Structural Concrete, Technical report, Fib Bulletin, no. 14, 2001.*
- [21] *ECP 203, Egyptian Code of Practice for Design and Construction of Concrete Structures, 2009.*
- [22] *ACI Committee, American Concrete Institute, & International Organization for Standardization, Building Code Requirements for Structural Concrete (ACI 318-05) and Commentary, American Concrete Institute, 2005.*
- [23] *BS 8110, Structural use of Concrete: Part 1: Code of Practice for Design and Construction, British Standard Institution, London, 1997.*
- [24] *JSCE. , Standard Specifications for Concrete Structures, Japan Society of Civil Engineers, Yotsuya 1-chome, Shinjuku-ku, Tokyo, 2007.*

Khaled Fawzy "Relative Study of Nonlinear Analysis for Torsional Strengthened RC Beams with Web Opening using CFRP and Steel Plates." IOSR Journal of Mechanical and Civil Engineering (IOSR-JMCE) , vol. 15, no. 1, 2018, pp. 65-78.